A peptide nucleic acid (PNA)-DNA ferrocenyl intercalator for electrochemical sensing

Houda Gaiji [a,b], *Pawan Jolly* [c], *Serife Ustuner* [c,d], *Sean Goggins* [d], *Manef Abderrabba* [b], *Christopher G. Frost* [d], *Pedro Estrela* [c]*

[a] Department of Chemistry, Faculty of Mathematical, Physical and Natural Sciences of Tunis, University Tunis El Manar, Tunis 2092, Tunisia
[b] Laboratory of Materials Molecules and Applications (LMMA), Preparatory Institute of Scientific and Technical Studies (IPEST), University of Carthage, La Marsa, Tunis 2070, Tunisia
[c] Department of Electronic & Electrical Engineering, University of Bath, Bath BA2 7AY, United Kingdom
[d] Department of Chemistry, University of Bath, Bath BA2 7AY, United Kingdom
* e-mail: p.estrela@bath.ac.uk

Abstract
A ferrocenyl intercalator was investigated to develop an electrochemical DNA biosensor employing a peptide nucleic acid (PNA) sequence as capture probe. After hybridization with single strand DNA sequence, a naphthalene diimide intercalator bearing ferrocene moieties (FND) was introduced to bind with the PNA-DNA duplex and the electrochemical signal of the ferrocene molecules was used to monitor the DNA recognition.
Electrochemical impedance spectroscopy was used to characterize the different modification steps. Differential pulse voltammetry was employed to evaluate the electrochemical signal of the FND intercalator related to its interaction with the complementary PNA-DNA hybrid. The ferrocene oxidation peaks were utilised for the target DNA quantification.
The developed biosensor demonstrated a good linear dependence of FND oxidation peak on DNA concentration in the range 1 fM to 100 nM of target DNA, with a low detection limit of 11.68 fM. Selectivity tests were also investigated with a non-complementary DNA sequence, indicating that the FND intercalator exhibits a selective response to the target PNA-DNA duplex.

Keywords: PNA, DNA, DNA-intercalator, ferrocenyl naphthalene diimide, DPV

1. Introduction

DNA-based biosensors have been involved in a wide range of applications such as medical diagnosis [1], agricultural and food sciences [2], gene sequences analysis [3] and environmental hazards control [4] using different transduction modes such as light sensitive, frequency, electronic and electrochemical based techniques [5-7]. Among them, electrochemical DNA biosensors present an attractive route for synergizing the biological recognition process and the transduction event, with the advantages of fast, specific, sensitive, and inexpensive detection system. In order to make such devices viable, researchers continuously try to develop methods that simplify the sensor construction and improve its sensitivity, selectivity and robustness.

An electrochemical DNA sensor is typically based on the binding ability of a nucleic acid layer with a complementary target DNA sequence. Various types of oligonucleotides have been used by researchers as probe molecules to selectively capture a DNA target; these probes include single-stranded DNA [8], hairpin DNA [9], locked nucleic acid (LNA) [10] and peptide nucleic acid (PNA) [11], which are grafted to the substrate surface via physical or electrochemical adsorption, self-assembly immobilization, biotin–avidin interactions, entrapment methods or covalent attachment [12,13].

In the past years, numerous strategies have been suggested for the development of electrochemical DNA sensors [14], including label free methods directly based on inherent electroactivity of some nucleotides [15,16], and indirect label-based methods which involve the use of electroactive markers and labels such as enzymes, nanoparticles, quantum dots, and redox indicators and intercalators mainly derived from organic dyes, anticancer or antibiotic drugs and metal complexes [17-20]. Of these

types of configuration, the widely adopted ones employ electroactive indicators containing organometallic or organic moieties which connect directly and selectively to the oligonucleotide sequences by electrostatic, groove binding or intercalating ways [19b]. Such intercalators, defined as organic small sized DNA binding molecules with an appropriate chemical structure, *e.g.* methylene blue, daunomycin, anthraquinone, ethidium bromide and ferrocenyl naphthalenediimide [20-24], present characteristic structures with a planar polycyclic ring, allowing them to fit between adjacent base pairs of the double helix structure without destroying hydrogen bonds. In fact, naphthalene planar core in FND molecule slides by perpendicular insertion between DNA-duplex base pairs and its two peripheral substituents are projecting out of the DNA grooves. The resulted FND-DNA complex is stabilized by non-covalent interactions which implicate catenane formation, π stacking and van der Waals forces, with a high rigidity and slow dissociation properties [22].

The special affinity of these intercalators to ds-DNA has been exploited to develop sensing systems that discriminate between single stranded and double stranded DNA sequences, as well as for monitoring the DNA hybridization process basing on the recognition and selection of the intercalator to the duplex structure [19a]

Here, we propose the study of the analytical application of a double stranded DNA intercalator derived from naphthalene diimide (N,N′-((((((1,3,6,8-tetraoxo-1,3,6,8-tetrahydrobenzo[lmn] [3,8]phenanthroline-2,7-diyl) bis(ethane-2,1-diyl)) bis(oxy)) bis(ethane-2,1-diyl)) bis(oxy)) bis(ethane-2,1-diyl)) diferrocenamide) for monitoring DNA hybridization using peptide nucleic acid (PNA) probes. This small organic molecule benefits from the redox activities of the two ferrocene (Fc) moieties, and the structural features of the naphthalene diimide core, in particular its chemical stability, planarity and high aptitude to interact with nucleic acid sequences via π– π stacking interactions [25] that make it suitable as a DNA binder. Unlike previous reports about the use of this Fc-bearing naphthalenediimide intercalator [26], this study examines the use of the intercalator in PNA-DNA interactions (see schematic in Figure 1), based on the advantages of PNA oligonucleotides as a capture probe, specifically a high biochemical stability and recognition specificity and an excellent binding affinity [11b]. It is interesting to notice that to date no DNA intercalator has been used for electrochemical monitoring of PNA-DNA hybridization.

2. Experimental

2.1. Reagents

Thiol terminated single-stranded PNA oligonucleotides (HS-$(CH_2)_6$-TTT AGG GAT TCC TGG GAA AA) were synthesized by Cambridge Research Biochemical (UK). The complementary ss-DNA 3'-TCC CTA AGG ACC CTT TTT GAC CTG-5', and a control DNA sequence 3'-AAA TGC CTA TAG ACC CTT GAC CTG-5' were obtained from Sigma Aldrich, UK. Unless otherwise stated, all chemicals were purchased from Sigma-Aldrich (UK) and used as received. Stock solutions of PNA and DNA nucleotides were prepared following the manufacturer's instructions and kept frozen for storage. All other used chemicals were of analytical grade and purchased from Sigma-Aldrich, UK. All aqueous solutions were prepared using 18.2 MΩ.cm ultra-pure water from a Milli-Q system (Millipore, USA).

2.2. Electrochemical characterization

Electrochemical measurements were performed using either a μAutolab III / FRA2 potentiostat (Metrohm Autolab, The Netherlands) or a CompactStat potentiostat (Ivium Technologies, The Netherlands) with a three-electrode system consisting of a platinum (Pt) counter electrode (ALS, Japan), Ag/AgCl (KCl) or Hg/Hg_2SO_4 (K_2SO_4) reference electrodes (BASi, USA) and a gold working electrode (CH Instruments, USA). All measurements were performed at room temperature.

Electrochemical impedance spectroscopy (EIS) experiments were carried out in 10 mM phosphate buffer (PB, pH 7.0) containing 2 mM $K_4[Fe(CN)_6]$ and 2 mM $K_3[Fe(CN)_6]$, using the μAutolab analyser and an Ag/AgCl reference electrode. The reference electrode was connected via a salt bridge filled with 50 mM PB and 100 mM K_2SO_4 (pH 7.0). The impedance spectrum was measured over the frequency range from 100 kHz to 100 mHz, with a 10 mV a.c. voltage superimposed on a d.c. bias of 0.195 V vs Ag/AgCl, corresponding to the formal potential of the redox couple.

The capacitance characterization was performed using the CompactStat equipment and a Ag/AgCl reference electrode connected via a salt bridge (10 mM PB, pH 7.4). The impedance measurements were operated in 10 mM phosphate buffer (pH 7.4) in a frequency range from 100 kHz to 100 mHz, with a 10 mV a.c. voltage superimposed on a bias d.c. voltage of 0 V [27].

Ferrocene peaks were monitored using differential pulse voltammetry (DPV) in 100 mM PB (pH 7.4) as supporting electrolyte. DPV scans were monitored between -0.2 V

and 0.7 V *vs.* Ag/AgCl with the scan rate of 0.05 Vs^{-1}. The FND intercalator was characterized using screen printed carbon graphite electrodes (GM Nameplate, Seattle, USA) via electrochemical methods for stability studies using DPV and cyclic voltammetry (CV)

2.3. Synthesis of the DNA intercalator

The Fc ds-DNA intercalator N,N′-((((((1,3,6,8-tetraoxo-1,3,6,8-tetrahydrobenzo[lmn][3,8]phenanthroline-2,7-diyl)bis(ethane-2,1-diyl))bis(oxy)) bis (ethane-2,1-diyl)) bis(oxy)) bis(ethane-2,1-diyl)) diferrocenamide was synthesised using a previously described protocol by Z. Yang *et al.* [26b]. Briefly, ferrocenecarboxylic acid was first treated with oxalyl chloride at 0 °C in dry dichloromethane. The result solid was then added to a solution of 2,2'-(ethylenedioxy)bis(ethylamine) under cold and anhydrous conditions to obtain N-(2-(2-(2-aminoethoxy)ethoxy)ethyl)-2-ferrocenamide. The obtained ferrocenylamide was reacted in a pressure-tight microwave reaction vial with 1,4,5,8-naphthalenetetracarboxylic dianhydride in anhydrous dimethylformamide followed by adding anhydrous triethylamine and sonicating the solution until homogenisation (approx. 15 min). The reaction mixture was finally heated at 140 °C for 5 min under microwave irradiation and the result product Fc-naphthalenediimide intercalator (FND) was extracted, purified and characterized employing common analytical methods [26b].

2.4. Fabrication of PNA-based biosensor

Gold disk working electrodes with a radius of 1.0 mm were mechanically polished with 0.3 µm aluminium oxide particles (Buehler, USA) on a polishing pad (Buehler) for 5 minutes. Electrodes were then rinsed with excess water followed by sonication in ultra-pure water to remove any remaining residues. Thereafter, electrodes were immersed in freshly prepared piranha solution (H_2SO_4/H_2O_2, v/v 7/3) for 5 minutes followed by rinsing thoroughly with Milli-Q water, to remove any residues of acids used.

The gold electrodes were then electrochemically cleaned in a classical three-electrode cell configuration by immersing them in a H_2SO_4 (0.5 M) solution and the potential was scanned between the oxidation and reduction potentials of gold, 0 V and +1.5 V *vs.* Ag/AgCl, with a scan rate of 0.2 V/s for 50 cycles until there was no further changes in the voltammograms. Finally, the cleaned gold electrodes were thoroughly rinsed with ultra-pure water, dried in a nitrogen stream and immediately subjected to a PNA immobilization solution.

The clean electrode surfaces were exposed to an optimized ratio of (1:5) thiolated PNA to 6-mercapto-1-hexanol (MCH) solution for the overnight preparation of a compact SAM layer [11a]. The use of a short-chain thiol spacer, such as MCH, is commonly adopted to reduce non-specific adsorption via the hydroxyl groups of MCH and to assure a "stand up" position of the PNA sequence [14b]. The PNA samples were prepared in a solution containing dimethyl sulfoxide (DMSO) and ultra-pure water [50% and 50% (v/v)] and heated to 50 °C for 10 min, before mixing with MCH. Concentrated solutions of MCH were prepared in pure ethanol and further diluted to the desired concentrations in the DMSO-water mixture.

After immobilization, electrodes were rinsed with ultra-pure water to remove any non-specific bounds thiols. In order to ensure complete thiol coverage of the gold surface, the electrodes were thereafter backfilled with 1 mM MCH prepared in 10 mM PB for 1h. Finally, the modified electrodes were carefully rinsed with water, and left in 10 mM PB (pH 7.0) for an hour for stabilization before the binding studies.

2.5. DNA Hybridization

For the DNA hybridization study, the fabricated PNA modified electrodes were incubated for 30 min with a 40 µl drop of different concentrations of DNA solution (complementary or non-complementary DNA sequences) prepared in 10 mM PB (pH 7.0). The electrodes were then carefully washed to remove non-specifically bound DNA and kept in PB solution for further use. The hybridization step of ss-DNA was characterized using EIS.

To monitor the hybridization event, the Fc-naphthalenediimide intercalator (FND) was employed and its binding behaviour with PNA-DNA duplex was investigated. For that, the above hybridized electrodes were incubated with a 20 µL of intercalator solution (1 mM, 50% DMSO in MilliQ water (v/v) for 30 minutes at room temperature. Then, the resulting electrodes were carefully rinsed and later analysed using electrochemical measurements (Figure 1).

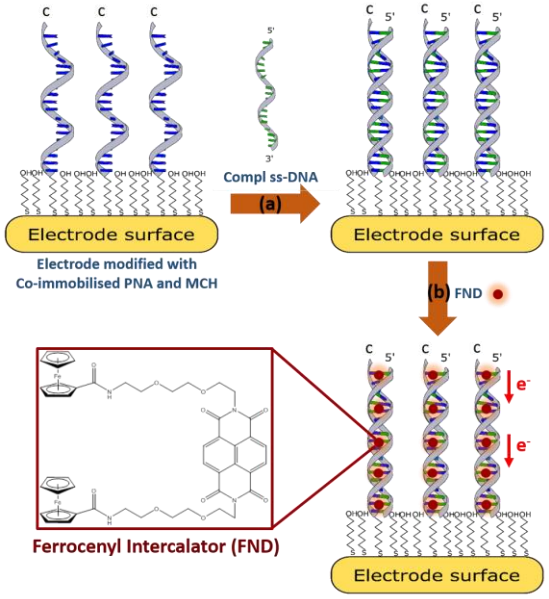

Fig. 1. Schematic illustration of the FND based biosensor for investigation of PNA-DNA hybridization: (a) PNA-DNA hybridization step, (b) FND binding with PNA-DNA duplex.

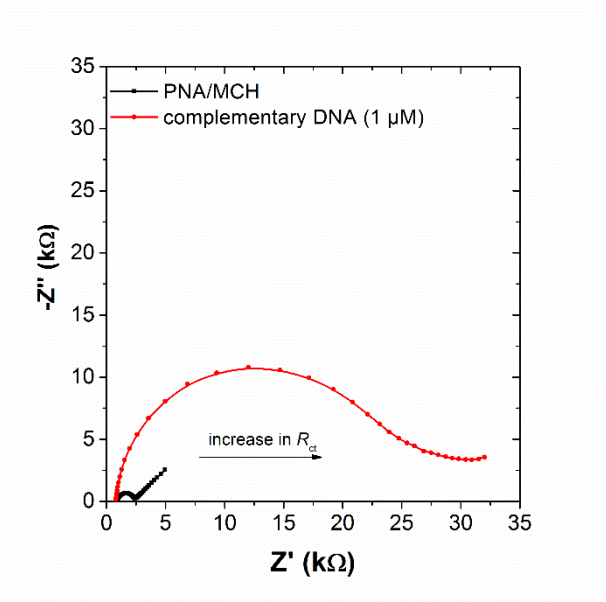

Fig. 2. EIS characteristics for PNA/MCH functionalized electrode before and after incubation with 0.1 µM complementary ss-DNA. Electrode prepared with PNA (2 µM) / MCH (10 µM); EIS measured with 2 mM $K_4[Fe(CN)_6]$ + 2 mM $K_3[Fe(CN)_6]$ in 10 mM PB (pH 7.0).

3. Results and discussion

3.1. Electrochemical characterization of DNA hybridization

The performance of the biosensor is directly related to the success of the different fabrication steps, namely the immobilization of thiolated PNA probes on the gold electrode and the DNA hybridization steps. In our work, EIS in Faradaic mode was employed for the characterization of the biosensor surface at different fabrication and molecular recognition steps.

Figure 2 presents a typical EIS behaviour of the PNA/MCH immobilized gold electrode, before and after DNA hybridization. From the Nyquist plots, the relatively neutral PNA-MCH monolayer shows a small electron charge transfer resistance (R_{ct}) of 1.42 kΩ (black curve). Such an observation could be attributed to neutral PNA molecules demonstrating a physical barrier to the negatively charged markers. After hybridization with the complementary DNA sequence, a significant increase of R_{ct} to 24.75 kΩ was observed. This augmentation could be associated to an increased electrostatic barrier to the negatively charged redox couple $[Fe(CN)_6]^{3-/4-}$ due to the negatively charged attached DNA.

3.2. Electrochemical characterization of FND intercalator

The synthesized compound was examined for its solubility in different solvents. The FND molecule was found to be insoluble in acetonitrile (C_2H_3N) and water (H_2O) but soluble in chloroform ($CHCl_3$) and dimethyl sulfoxide (DMSO). The synthesized FND was characterized by high resolution mass spectrometer (HRMS) using an electrospray time-of-flight MicroTOF spectrometer (Supplementary Information, Figure S-2). The positive ESI spectrum indicated the presence of the intercalator at 975.1914 m/z which corresponds to the molecular weight of the dsDNA Fc-intercalator, $C_{48}H_{48}N_4O_{10}Fe_2$, with sodium (975.1961), which is in accordance with previously published data [26b].

The oxidation potential of the FND binder was electrochemically characterized by using DPV in different concentrations from 0.004 mM to 1 mM in PBS buffer. It could be clearly seen that the peak current decreases with decreasing concentration of FND intercalator (supporting information, Figure S-3). The average oxidation potential was calculated to be 0.34 + 0.02 V *vs.* Ag/AgCl. The value obtained is slightly lower that what is reported in the literature [26b]. Such a difference could be due to the fact that the measurements were performed in a solution of FND intercalator using clean bare gold electrodes. Cyclic Voltammetry was also performed to understand the

reversibility of the reaction with FND-intercalator (supporting information, Figure S-4. From the CV measurements, a reversibility factor of 0.81 + 0.05 was obtained, which demonstrates a nearly reversible system.

The stability of the FND binder was also tested at different storage temperatures. 0.1 mM FND intercalator solution was stored at -20˚C, 4˚C and 21˚C and the oxidation potential was monitored over 10 days. The data presented in Figure 3 shows the oxidation peak potential taken from the DPV results (supplementary information, Figure S-6). It can be clearly seen that the best stability conditions were obtained for -20˚C, where a negligible shift in the peak potential was observed over a 10-day period. Hence, for the experiments FND was stored at -20˚C before use.

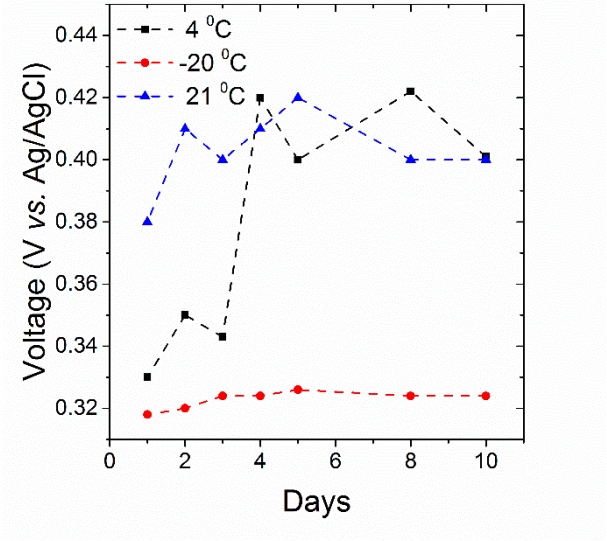

Fig. 3. Stability at three different storage conditions. Oxidation potential peak for FND at 21°C (a). 4°C (b) and -20°C (c).

3.3. Investigation of the FND–hybridized probe binding

In order to demonstrate the interaction between FND molecules and the PNA-DNA duplex, EIS in non-Faradaic mode was used to monitor the changes in capacitance of the system before and after incubation with the ferrocenyl compound. After each electrode modification steps, a non-Faradaic EIS measurements were performed in 10 mM phosphate buffer (pH 7.4), without the use of any redox markers. A Cole-Cole plot was obtained as shown in Figure 4, from the EIS data by defining a complex capacitance as $C^*=C'+jC''=1/j\omega Z$, as described by Jolly *et al.* [27]. It can be seen that the use of the FND binder (blue curve) induces a remarkable increase in the capacitance due to the perturbation of the dielectric interface, which attest the successful attachment of FND molecules to the PNA-DNA duplex.

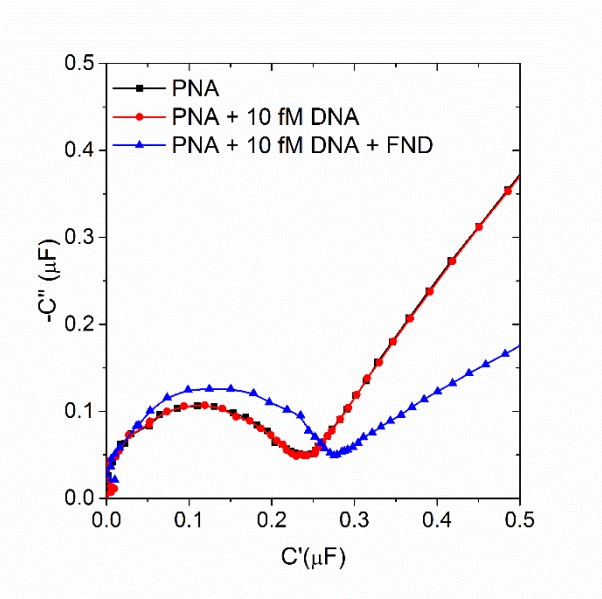

Fig. 4. Cole-Cole plot representing capacitance of the system for PNA/MCH functionalized electrode incubated with 10 fM complementary ss-DNA and 1 mM FND binder. EIS measured in 10 mM phosphate buffer (pH 7.4).

3.4. Analytical performance with FND intercalator

To monitor the significance of the FND binder to generate a simple and rapid electrochemical response related to the PNA–DNA hybridization, a DPV technique has been employed. Thereby, the modified electrodes were subjected to a DPV measurement in the potential range of -0.2 to 0.7 V in 100 mM PB, after incubation with fixed concentrations of FND. A well-defined peak appears at 0.49 V *vs.* Ag/AgCl, corresponding to the oxidation of the ferrocene moieties on the electrode surface (see inset of Figure 5). Such an observation, is in accordance with previous work reported for DNA-DNA hybridization [26].

Comparing the DPV voltammograms of the FND binder in the presence and the absence of complementary DNA, confirms that the peak current is attributed to the hybridization phenomenon, and prove a significant interaction only between the oligonucleotides duplex (PNA-DNA) and the electroactive ferrocenyl DNA intercalator. This observation is in favour of the use of our detection system for the monitoring DNA hybridization event. A high peak current of 1.5 µA was obtained with 1 fM DNA concentration, while a negligible signal was observed with a blank DNA concentration.

A dose response is presented in Figure 5. The peak currents of FND increase proportionally with the target DNA concentration: the larger amount of DNA is functionalized on the PNA probe, the more PNA-DNA hybrids are formed, the more FND molecules bind to the duplex, most likely through intercalation, and the superior electrochemical signal is generated. The measured DPV signals demonstrate a logarithmic dependence with the concentration of complementary DNA. The calibration curve exhibits a good linearity between 1 fM and 100 nM of DNA with regression equation $i_{pa} = 1.19 \times 10^{-7} \log(c_{DNA}) + 1.60 \times 10^{-7}$ (i_{pa} in µA and c_{DNA} in fM) and correlation coefficient R^2=0.98217. The limit of detection (LOD) calculated from the 3S/N ratio is 11.68 fM, indicating a good sensitivity of the DNA biosensor.

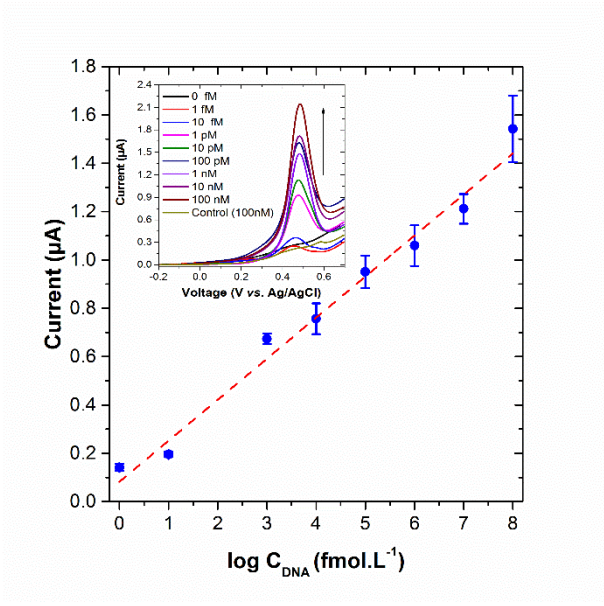

Fig. 5. Current peak height change upon incubation with 1 mM FND intercalator, as a function of ss-DNA concentration. Electrode prepared with PNA (2 µM) /MCH (10 µM). DPV measurement conditions: scan range -0.2 V to 0.7 V *vs.* Ag/AgCl; step potential 5 mV; scan rate 50 $mV.s^{-1}$; supporting electrolyte 100 mM PB (pH 7.4). The error bars indicate standard mean error from independent samples.

Specificity is a fundamental aspect in DNA sensors. To verify the specificity of the biosensor, we performed a specificity test with a non-complementary DNA sequence using the same intercalator binding scheme. The inset of Figure 5 shows the DPV signal for an electrode incubated with a large concentration (100 nM) of the non-complementary sequence and 1 mM of FND solution. The data shows that the introduction of the non-complementary DNA to the PNA-functionalized surface, even with high concentration levels, does not induce a responsive current. It confirms that the developed sensor exhibits a satisfactory specificity towards the complementary DNA due to high specific interaction between the FND intercalator and the probe-target hybrid.

4. Conclusions

Taking the advantages of the excellent recognition specificity of peptide nucleic acid and the special affinity of naphthalene diimide DNA intercalator to double stranded nucleotide sequences, a simple and high sensitive electrochemical DNA biosensor is obtained. A self-assembled PNA monolayer immobilized onto gold electrode surface was used for the detection of single strand DNA sequences exploiting the electrochemical signal of accumulated ferrocenyl-bearing DNA intercalators. The obtained results demonstrate that the used naphthalene diimide intercalator bind specifically to the PNA-target DNA duplex and the developed biosensor shows a potential simple and specific sensing system with a low detection limit in the femtomolar level. This newly developed sensing strategy introduce a promising platform for monitoring DNA hybridization using PNA probes and ferrocenyl-containing DNA threading intercalators.

Acknowledgements

P.J. was funded by the European Commission FP7 Programme through the Marie Curie Initial Training Network PROSENSE (grant no. 317420, 2012-2016). S.U. is funded by the EPSRC Centre for Doctoral Training in Sustainable Chemical Technologies.

References

[1] a) J. Wang, *Biosens. Biolectron.* **2006**, *21*, 1887-1892; b) V. Gubala, L. F. Harris, A. J. Ricco, M. X. Tan, D. E. Williams, *Anal. Chem.* **2012**, *84*, 487-515.

[2] a) D. S. Elenis, D. P. Kalogianni, K. Glynou, P. C. Ioannou, T. K. Christopoulos, *Anal. Bioanal. Chem.* **2008**, *392*, 347-354; b) L. Monaci, A. Visconti, *Trends Food Sci. Tech.* **2010**, *21*, 272-283.

[3] a) O. Panke, A. Kirbs, F. Lisdat, *Biosens. Bioelectron.* **2007**, *22*, 2656-2662; b) S. N. Topkaya, B. Kosova, M. Ozsoz, *Clin. Chim. Acta* **2014**, *429*, 134-139.

[4] a) I. Palchetti, M. Mascini, *Analyst* **2008**, *133*, 846-854; b) J. Zhang, Y. Tang, L. Teng, M. Lu, D. Tang, *Biosens. Biolectron.* **2015**, *68*, 232-238.

[5] a) K. H. Lee, J. O. Lee, M. J. Sohn, B. Lee, S. H. Choi, S. K. Kim, J. B. Yoon, G. H. Cho, *Biosens. Bioelectron.* **2010**, *26*, 1373-1379; b) B. Cai, S. Wang, L. Huang, Y. Ning, Z. Zhang, G. J. Zhang, *ACS Nano* **2014**, *8*, 2632-2638; c) Y. Du,

B. J. Lim, B. Li, Y. S. Jiang, J. L. Sessler, A. D. Ellington, *Anal. Chem.* **2014**, *86*, 8010-8016.

[6] W. W. Zhao, J. J. Xu, H. Y. Chen, *Chem. Rev.* **2014**, *114*, 7421-7441.

[7] A. Bertucci, A. Manicardi, A. Candiani, S. Giannetti, A. Cucinotta, G. Spoto, M. Konstantaki, S. Pissadakis, S. Selleri, R. Corradini, *Biosens. Bioelectron.* **2015**, *63*, 248-254.

[8] a) V. Dharuman, K. Vijayaraj, S. Radhakrishnan, T. Dinakaran, J. S. Narayanan, M. Bhuvana, J. Wilson, *Electrochim. Acta* **2011**, *56*, 8147-8155; b) H. Gao, X. Qi, Y. Chen, W. Sun, *Anal. Chim. Acta* **2011**, *704*, 133-138.

[9] a) J. Chen, J. Zhang, H. Yang, F. Fu, G. Chen, *Biosens. Bioelectron.* **2010**, *26*, 144-148; b) A. Abi, E. E. Ferapontova, *Anal. Bioanal. Chem.* **2013**, *405*, 3693-3703.

[10] a) S. Laschi, I. Palchetti, G. Marrazza, M. Mascini, *Bioelectrochemistry* **2009**, *76*, 214-220; b) K. Wang, Z. Sun, M. Feng, A. Liu, S. Yang, Y. Chen, X. Lin, *Biosens. Bioelectron.* **2011**, *26*, 2870-2876.

[11] a) S. D. Keighley, P. Estrela, P. Li, P. Migliorato, *Biosens. Bioelectron.* **2008**, *24*, 906-911; b) C. Briones, M. Moreno, *Anal. Bioanal. Chem.* **2012**, *402*, 3071-3089.

[12] a) A. Sassolas, B. D. Leca-Bouvier, L. J. Blum, *Chem. Rev.* **2008**, *108*, 109-139; b) S. Cagnin, M. Caraballo, C. Guiducci, P. Martini, M. Ross, M. SantaAna, D. Danley, T. West, G. Lanfranchi, *Sensors* **2009**, *9*, 3122-3148.

[13] M. M. Rahman, X. B. Li, N. S. Lopa, S. J. Ahn, J. J. Lee, *Sensors* **2015**, *15*, 3801-3829.

[14] a) J. Wang, *Anal. Chim. Acta* **2002**, *469*, 63-71; b) E. Palecek, M. Bartosik, *Chem. Rev.* **2012**, *112*, 3427-3481.

[15] J. Wang, A. N. Kawde, *Anal. Chim. Acta* **2001**, *431*, 219-224.

[16] D. O. Ariksoysal, H. Karadeniz, A. Erdem, A. Sengonul, A. A. Sayiner, M. Ozsoz, *Anal. Chem.* **2005**, *77*, 4908-4917.

[17] a) M. Pumera, M. T. Castaneda, M. I. Pividori, R. Eritja, A. Merkoçi, S. Alegret, *Langmuir* **2005**, *21*, 9625-9629; b) A. Merkoçi, M. Aldavert, S. Marin, S. Alegret, *Trends Anal. Chem.* **2005**, *24*, 341-349.

[18] J. Pan, *Biochem. Eng.* **2007**, *35*, 183-190.

[19] a) M. Fojta, L. Havran, H. Pivokova, P. Horakova, M. Hocek, *Curr. Org. Chem.* **2011**, *15*, 2936-2949; b) E. E. Ferapontova, *Curr. Anal. Chem.* **2011**, *7*, 51-62.

[20] M. Y. Wei, L. H. Guo, P. Famouri, *Microchim. Acta* **2011**, *172*, 247–260.

[21] a) S. Takenaka, K. Yamashita, M. Takagi, Y. Uto, H. Kondo, *Anal. Chem.* **2000**, *72*, 1334-1341; b) Z. Gao, N. Tansil, *Anal. Chim. Acta* **2009**, *636*, 77-82; c) S. Sato, A. Hirano, S. Takenaka, *Anal. Chim. Acta* **2010**, *665*, 91-97; d) S. Sato, S. Takenaka, *Anal. Sci* **2012**, *28*, 643-649.

[22] N. C. Tansil, E. A. B. Kantchev, Z. Gao, H. Yu, *Chem. Commun.* **2011**, *47*, 1533-1535.

[23] S. Watanabe, S. Sato, K. Ohtsuka, S. Takenaka, *Anal. Chem.* **2011**, *83*, 7290-7296.

[24] M. Gebala, W. Schuhmann, *Phys. Chem. Chem. Phys.* **2012**, *14*, 14933–14942.

[25] M. Pandeeswar, T. Govindaraju, *J. Inorg. Organomet. Polym.* **2015**, *25*, 293-300.

[26] a) Z. Yang, B. Kasprzyk-Hordern, S. Goggins, C. G. Frost, P. Estrela, *Analyst* **2015**, *140*, 2628-2633; b) Z. Yang, M. A. d'Auriac, S. Goggins, B. Kasprzyk-Hordern, K. V. Thomas, C. G. Frost, P. Estrela, *Environ. Sci. Technol.* **2015**, *49*, 5609-5617.

[27] P. Jolly, N. Formisano, J. Tkáč, P. Kasák, C. G. Frost, P. Estrela, *Sens. Actuators B* **2015**, *209*, 306-312.